Charging Load Pattern Extraction for Residential Electric Vehicles: A Training-free Non-intrusive Method

Yue Xiang, *Senior Member, IEEE*, Yang Wang, Shiwei Xia, *Senior Member, IEEE*, Fei Teng, *Member, IEEE*

***Abstract*— Extracting the charging load pattern of residential electric vehicle (REV) will help grid operators make informed decisions in terms of scheduling and demand-side response management. Due to the multi-state and high-frequency characteristics of integrated residential appliances from the residential perspective, it is difficult to achieve accurate extraction of the charging load pattern. To deal with that, this paper presents a novel charging load extraction method based on residential smart meter data to noninvasively extract REV charging load pattern. The proposed algorithm harnesses the low-frequency characteristics of the charging load pattern and applies a two-stage decomposition technique to extract the characteristics of the charging load. The two-stage decomposition technique mainly includes: the trend component of the charging load being decomposed by seasonal and trend decomposition using loess (STL) method, and the low-frequency approximate component being decomposed by discrete wavelet technology (DWT). Furthermore, based on the extracted characteristics, event monitoring, and dynamic time warping (DTW) is applied to estimate the closest charging interval and amplitude. The key features of the proposed algorithm include (1) significant improvement in extraction accuracy; (2) strong noise immunity; (3) online implementation of extraction. Experiments based on ground truth data validate the superiority of the proposed method compared to the existing ones.**

***Index Terms*—Residential electric vehicle, non-intrusive load extracting, two-stage decomposition, ant-identification analysis, smart meter**

NOMENCLATURE

Abbreviations

REV	Residential electric vehicle
EV	Electric vehicle
AC	Air conditioner
ILE	Intrusive load extracting
NILE	Non-intrusive load extracting
STL	Seasonal and trend decomposition using loess
DWT	Discrete wavelet technology
DTW	Dynamic time warping
EACL	Exploratory analysis of charging load
FP	False positive
TP	Ture positive
FN	False negative
PRE	Precision
REC	Recall rate
SNR	Signal to noise ratio

Indices

t	Time
m	Index for extracted charging load patterns
j	Index for residential appliances
α	Index for layers in DWT
k	Index for any path in DTW

Parameters

$\boldsymbol{D}$	Dictionary library related to REV
x_{EV}	Extracted EV charging load pattern
x_L	Low-frequency component related to REV
x_H	High-frequency component related to REV
x_O	Residual component
x	Smart meter data
x_{ap}	Residential appliances without EV
x_{tr}	Trend component
x_{se}	Seasonal component
x_{re}	Residual component
$x_{L,\alpha}$	Low-frequency component of layer α
$x_{H,\alpha}$	High-frequency component of layer α
S	Rated power vector of charging load
M	Total number of selectable related power
x_{opt}	Selectable charging load patterns
w_t	Robustness weight at time t
η	Minimum difference value
ε	Threshold to determine charging event
Dur_{min}	Minimum charging duration
Dur_{max}	Maximum charging duration
$E_{interval}$	Charging interval vector from start time to end time
$\boldsymbol{\Theta}$	Maximum number of the charging duration
$\boldsymbol{O}$	Similarity distance matrix by DTW

This work is carried out during Yue Xiang's visit at Imperial College London and supported by the China State Key Laboratory of Alternate Electrical Power System with Renewable Energy Sources (Grant No. LAPS20011), UK EPSRC Supergen Energy Networks Hub (EP/S00078X/1) and International Visiting Program for Excellent Young Scholars of Sichuan University. (*corresponding author: Fei Teng.*)

Yue Xiang is with the College of Electrical Engineering, Sichuan University, Chengdu 610065, China (e-mail: xiang@scu.edu.cn). Yang Wang is with the Powerchina Sichuan Electric Power Engineering Co., Ltd, Chengdu 610065, China (e-mail: yangwangstu@outlook.com). Shiwei Xia is with the State Key Laboratory of Alternate Electrical Power System with Renewable Energy Sources, North China Electric Power University, Beijing 102206, China (e-mail: s.w.xia@ncepu.edu.cn). Fei Teng is with the Department of Electrical and Electronic Engineering, Imperial College London, London SW7 2AZ, U. K. (e-mail: f.teng@imperial.ac.uk).

I. INTRODUCTION

At present, the depletion of fossil energy and environmental problems are becoming increasingly challenging. As a means of transportation using clean energy, EVs are bound to achieve rapid development and large-scale applications [1]. The electric industry expects the penetration rate of EVs in the US will reach 29% by 2030 [2]. However, the large-scale roll-out of EVs will have a significant impact on power grid reliability and stable operation [3]. These negative effects mainly depend on charging behaviors [4], [5]. Thus, the effective identification of possible EV charging load pattern

would be a crucial part before significantly dealing with the potential "negative" impacts and "positively" utilization of large-scale EV energy resources from the demand side.

An intrusive load extracting method (ILE) that captures EV charging behaviors by installing monitoring devices at home is often unrealistic [6], due to the additional hardware installation costs and the leakage of residential energy privacy. Therefore, the non-intrusive load extracting (NILE) methods that extract the residential charging load patterns from smart meter have attracted growing interest [7]. The key idea for NILE is to capture the characteristics related to the charging load from the smart meter, and further realize the extraction of the charging load pattern. Currently, the methods for non-intrusive load monitoring include mainly signal processing and machine learning [8], [9]:

Signal processing: Some methods for extracting the characteristics from smart meter data to achieve load decomposition, such as factorial hidden Markov model (FHMM) [10], [11], independent principal component analysis (ICA) [12], and non-negative matrix factorization [13], have been widely investigated. With the rapid development of image recognition techniques, new load decomposition algorithms have appeared, such as sparse decomposition, and dictionary learning [14]. A common feature of the above algorithms is to learn a library for each charging load pattern and adopt the learned dictionary as a basis in the process of NILE [15]. However, due to the difference in charging power and charging behavior of EVs for different drivers, it is difficult to select a suitable charging load dictionary from the library.

Machine learning: The load pattern of a specific electrical appliance could be non-intrusively identified through enough data from the smart meter database. At present, lots of machine learning algorithms have been applied in NILE, such as convolutional neural networks [16], support vector machines [17], decision trees [18], and deep learning [19]. However, building a machine learning model requires a large amount of labeled training data (the charging load data cannot be obtained in practice) and the sensitive hyperparameter adjustments.

Extensive training and computation to capture the characteristics related to the charging load are the main limits of the aforementioned methods [20]. Besides, microelectronics and high-frequency switching loads from residential appliances e.g., microwave oven, laptop, and inverter air conditioners, will mask the characteristics of the charging pattern. The signal of the EV charging load has its strong characteristics that can be used to facilitate NILE. The charging load has two-state (on/off) and the switching frequency between the two states is very low. Therefore, the extraction of the REV charging load can be divided into three steps: 1) the signal rising point, 2) the signal steady-state interval, and 3) the signal falling point [20]. In [21], step 1) and step 3) are extracted by the skipping power difference, and a boundary box fitting algorithm is proposed further to extract step 2). However, other power events that can interfere with the charging load in step 2). In [5] and [22], a novel algorithm was designed to extract step 2), but the signals containing noise or multi-power appliances cannot be decomposed accurately [23]. The novel NILE algorithms are needed to be designed or improved to overcome the sample data bottleneck, eliminate high-frequency interference, and promote computational efficiency.

To deal with the limitation in the above studies, a novel non-intrusive charging load extraction algorithm would be proposed. A two-stage decomposition technology would be built in the method to extract the characteristics related to the charging load for effectively filtering out the high-frequency components, in which the trend component of the charging load being decomposed by STL, and the low-frequency approximate component being decomposed by DWT would be investigated. Then, the skipping power difference would be considered to be adopted to extract the rising and falling points of charging behavior. Besides, DTW is used to calculate the closest charging amplitude. To accommodate the requirements of NILE, probabilistic statistical results of charging behavior (charging interval, amplitude) will be introduced as boundary constraints for personalized extraction.

Compared with existing ones, the proposed method in this paper not only maintains the advantages of signal processing algorithm, including a low computational complexity and online extraction capabilities without explicit training step but also being expected with higher estimation accuracy when dealing with high-frequency, multi-state components with smart meter data due to the designed training-free algorithm, which could contribute to the charging pattern extraction of REV with stronger noise immunity, low computational cost capability.

The rest of the paper is organized as follows: Section II exploratively analyzes the characteristics of the charging load, the time-frequency characteristics, and the correlation with other electrical appliances. The proposed non-intrusive extraction method is established in Section III. Section IV verifies the effectiveness of the proposed algorithm with actual data. Finally, Section V concludes the paper.

II. Exploratory Analysis Of REV Charging Load

Residential smart meter data consists of energy consumption of various appliances, as shown in Fig. 1. Before designing the extraction algorithm, an exploratory analysis of the charging load (EACL) is performed. Thus, the charging behavior of REV and the time-frequency characteristics of other electric appliances are analyzed as follows.

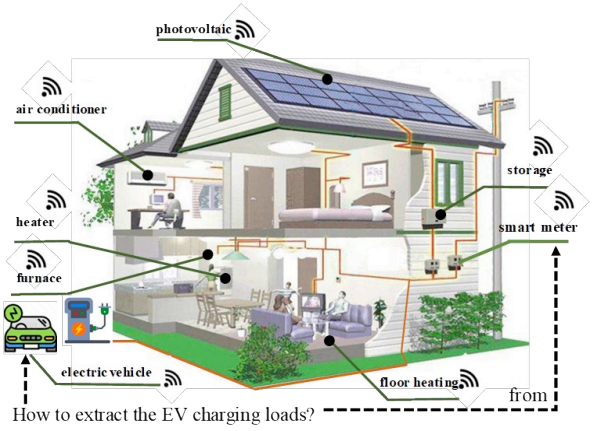

Fig. 1. Schematic diagram of residential electricity appliances

A. REV charging power and statistical features

The selected 1-min resolution smart meter data is derived from the Pecan Street demonstration data port [24]. There are five main types of REVs in this block, and their rated charging power ranges from 3 kW to 10 kW as shown in Table I. Furthermore, the profile shape of the charging load is approximately rectangular.

TABLE I
SELECTED REV TYPE AND CHARGING POWER

EV model	Charging power (kW)
Category I	3, 3.4, 3.6
Category II	6, 6.6, 6.8, 7.0, 7.2, 7.5
Category III	9.3, 10

Furthermore, the statistical analysis of residential charging load data from the same data port could indicate the statistical information of charging patterns' basic features, such as charging duration, the interval of adjacent charging events, and the number of charging events. The majority of charging durations of residential charging durations are more than 30 min while charging behavior rarely lasts more than 300 min. Moreover, the residents are unlikely to charge greater than three times a day, and the interval between two adjacent charging events is often greater than two hours. The above conclusions are consistent with the results using different data sources [25].

B. Power behavior analysis of residential appliances

Combined with the analysis of the REV charging durations in Section A, the power patterns of residential appliances and REV are analyzed to better extract the REV charging load pattern. The time-frequency characteristics of residential power devices for one day are shown in Fig. 2, while the resolution of the data is 1 min.

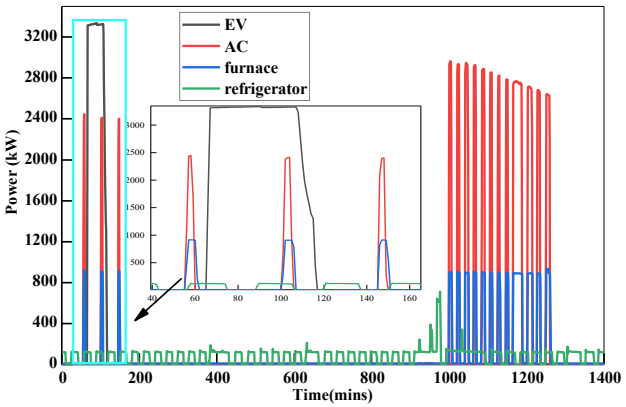

Fig. 2. Load profile of residential appliances

In Fig. 2, the rated charging power of AC is close to REV, and there could be an overlap with the pattern of AC during a small charging time (less than 30 min). Similar power patterns will interfere and increase the difficulty of non-intrusively extracting the target REV charging load pattern from the smart meter data. The furnace and AC have higher spike frequencies, and the interval between two adjacent peaks is small. Moreover, based on the duration of power behavior, it can be assumed that REV belong to the low-frequency signal. In contrast, it can be defined as the high-frequency signals for the furnace and AC. Besides, low-power consumption, such as refrigerators, can be defined as a steady-state signal. It is worth noting that the high-frequency and steady-state here are compared to the EV profile. For extracting the REV charging load patterns, it can be regarded as a process of denoising, which should filter out high-frequency noise signals, and combine the event exploration to further extract the charging load patterns. However, the superposition of power signals with different frequencies has become a bottleneck for extracting characteristics related to the charging load. To solve the above-mentioned problem, we design a two-stage decomposition algorithm in section III.

III. PROPOSED NON-INTRUSIVE EXTRACTION METHOD

A. Extraction problem formulation

For the smart meter data, it is assumed $x=[x_t,..,x_T]$, $t=1,\ldots, T$, which related to the non-intrusive extraction of REV charging load patterns. Thus, the process of extracting can be expressed as:

$$x_{EV} = x - \sum_{j=1}^{N} x_{ap,j} \tag{1}$$

$$x_{EV,m} = \boldsymbol{D} \cdot x \tag{2}$$

where N denotes the number of residential appliances without EVs; $x_{ap,j}$ represents the jth residential appliance; $x_{EV,m}$ denotes the mth charging load pattern that extracted from x, and $x_{EV,m}$ is a subset of x_{EV}.

Considering the low-frequency characteristics and high charging power amplitude of the REV charging load, the extraction problem can be transformed and formulated as:

$$x = x_L + x_H + x_O \tag{3}$$

$$x_{EV} = F(x_L) \tag{4}$$

where F denotes the corresponding extraction function.

B. Two-stage decomposition

For smart meter data containing multiple pulses and high-frequency noise, such as microwave ovens, laptops, and inverter AC. Therefore, the purpose of the two-stage is to eliminate interference (noise component, local abrupt), and the characteristic (x_L) that has the highest correlation with the charging load pattern can be obtained. How to obtain x_L is key to capture the charging load patterns. In this section, a two-stage decomposition technique will be introduced to obtain x_L, which is closely correlated with the charging load. In stage I, the STL method is first adopted to extract the trend component. In stage II, the DWT method is used to match the characteristic component related to the charging load.

1) Extracting the low-frequency trend component (stage I):

In this illustration, by adopting the STL method to extract trend component $x_{tr}=[x_{tr,t},\ldots, x_{tr,T}]$ from smart meter data, it is possible to explore the impact of the charging load on the trend of overall residential power consumption. STL technology is a signal decomposition method that uses robust local weighted regression as a smoother to decompose the smart meter data into a low-frequency trend, high-frequency residual, and seasonal component [26]. The advantage of STL is that it can robustly estimate the trend component without being distorted by the abnormal behavior in the data, which can help keep the particularity of the charging load during extraction. The formula of STL is:

$$x_t = x_{tr,t} + x_{se,t} + x_{re,t} \quad t = 1,\ldots,T \tag{5}$$

For smart meter readings, x_{tr} is often the low-frequency patterns (charging load), x_{se} describes the periodic character of the signal, such as refrigerator, x_{re} is more related to the high-frequency component of the signal, such as switching appliances, etc.

The process of STL includes two recursive parts: the inner loop and outer loop. The inner loop is mainly adopted to extract and update x_{tr}, and x_{se}, the outer loop is used to adjust the weights from the inner loop, which can reduce the impact of abnormal data on x_{tr}, x_{se}. When all weights are 1, the initial traversal of the outer loop is executed, and then k-th traversal of the outer loop is executed. For inner loop, let $x_{tr}(k)$ and $x_{se}(k)$ be the trend, seasonal components after the k-th loops, and sets $x_{tr}(1)=0$. The inner loop to update $x_{tr}(k)$, $x_{se}(k)$ can be divided into six steps:

Step 1: Remove trend component from smart meter data, $x_{dt}=x-x_{tr}(k)$. If the value of $x(t)$ is missing, then $x_{dt}(t)$ should be lost at time t.

Step 2: Perform LOESS smoothing on the periodic subsequence in x_{dt}(the period of the subsequence is T_{dt}). When all subsequences are smoothed, the sequence $c(k+1)$ of length $(T+2T_{dt})$ can be obtained.

Step 3: Perform low-pass filtering of length T_{dt}, T_{dt}, 3 on $c(k+1)$, and adopt LOESS smoothing to obtain sequence $l(k+1)$.

Step 4: Remove the trend and seasonal component of $c(k+1)$ at $(k+1)$ iteration to reduce the interference of low-frequency components to x_{se}, $x_{se}(k+1)=c(k+1)-l(k+1)$.

Step 5: Adopt LOESS regression for $x_{sd}(k+1)=x-x_{se}(k+1)$ to obtain $x_{tr}(k+1)$.

Step 6: Perform LOESS smoothing on x_{sd} to extract x_{tr}, and the smoothed sequence has no missing values. When x_{sd} is in the $k+1$ iteration, $x_{tr}(k+1)$ is the smoothed value.

In STL, the LOESS function is a local polynomial regression, which is essentially a process of smoothing the extracted trend component from smart meter data, and the specific mathematical derivation can be seen in [27]. To eliminate the influence of outliers on the LOESS regression results in the inner loop, it is necessary to define a robustness weight for each sampling point of x in the outer loop. This robustness weight can represent the maximum of x_{re}. When the outlier $|x_{re}|$ is very large, the corresponding weight value is close to 0. At time t, the robustness weight w_t can be expressed as:

$$w_t = \omega\left(\left| f(x_t) - x_{tr,t} \right| / h\right) \tag{6}$$

$$\omega(u) = \begin{cases} (1-u^2)^2 & 0 \le u < 1 \\ 0 & u \ge 1 \end{cases} \tag{7}$$

$$h = g \cdot median(|\, f(x_t) - x_{tr,t}\,|) \tag{8}$$

where, $f(x_t)$ donates trend component obtained due to outlier value of x_t; g presents the coefficient related to robustness weight, usually sets to 6. Based on the value of the outlier $|f(x_t)-x_{tr,t}|$ at x_t, the robustness weight (6) can be assigned.

2) Extracting the characteristics related to the REV (stage II)

Based on the trend component $x_{tr}=[x_{tr,t},\ldots,x_{tr,T}]$ obtained in stage I, DWT [28] is used to extract the characteristics of REV. The signal of different scales can be discretely decomposed by DWT, to capture the local time-domain characteristics.

The principle of DWT is to design low-pass and high-pass filters to decompose the original signal into features of different frequencies, as shown in Fig. 3.

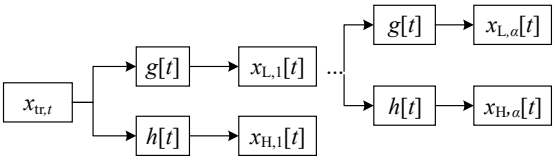

Fig. 3. The hierarchical structure of the DWT

where, $g[t]$, $h[t]$ represents the low-pass and high-pass filters, respectively. For the α-th architecture:

$$x_{L,\alpha-1}[t] = x_{L,\alpha}[t] + x_{H,\alpha}[t] \tag{9}$$

$$\begin{cases} x_{L,\alpha} = \sum_{k=0}^{K-1} x_{L,\alpha-1}[2t-k]g[k] \\ x_{H,\alpha} = \sum_{k=0}^{K-1} x_{L,\alpha-1}[2t-k]h[k] \end{cases} \tag{10}$$

where $K=T/2^{\alpha}$. The key to extracting the characteristics related to the charging load is to determine the $g[k]$, $h[k]$, and α. The scale function Harr in discrete wavelet is similar to the charging behavior of REV, hence Harr scale function is adopted as the mother wavelet (base) to extract charging characteristics, which is shown in the formula [28]:

$$\psi(t) = \phi(2t) - \phi(2t-1) \tag{11}$$

$$\phi(t) = \begin{cases} 1 & 0 \le t \le 1 \\ 0 & others \end{cases} \tag{12}$$

Therefore, Eq. (11) can be further transformed into:

$$\psi(t) = \sum a_l \phi(2t - l) \quad a_l \in R \tag{13}$$

In (10), t can be replaced with 2α-t-k, and the (10) can be transformed into:

$$\begin{cases} x_{L,\alpha} = \sum_{k \in K} b_k^{\alpha} \psi(2^{\alpha} t - k) \\ x_{H,\alpha} = \sum_{k \in K} a_k^{\alpha} \phi(2^{\alpha} t - k) \end{cases} \tag{14}$$

where:

$$\begin{cases} b_k^{\alpha} = (x_{\mathrm{L},\alpha} - x_{\mathrm{L},\alpha+1})/2 \\ a_k^{\alpha} = (x_{\mathrm{L},\alpha} + x_{\mathrm{L},\alpha+1})/2 \end{cases} \tag{15}$$

DWT is used to decompose the time-series components from the stage I, which can extract the characteristic component $x_{\alpha,L}$ directly related to REV. If the correlation between $x_{L,\alpha}$ and the charging load is highest, then $x_{L,\alpha}$ can be considered as the component that is required in the proposed algorithm.

C. Monitoring and matching of REV charging event

Based on the extracted characteristic $x_{L,\alpha}$ related to the charging load, the charging start, and end time can be determined by monitoring the signal edge. Besides, the amplitude of the charging load could be matched by the DTW method. For the proposed method, the implementation process monitoring and matching of REV charging events do not rely on actual charging data, and not require training data, which is training-free.

1) Edge monitoring of REV charging event

According to $x_{L,\alpha}$ extracted by the two-stage decomposition, we further extract the charging load pattern. And the complete charging behavior is symmetrical at the center point between the initial charging point t^+ and the end charging point t^-. Therefore, the edge $[t^+, t^-]$ can be identified according to the high-order difference of the power sampling point.

$$\Delta x_{L,\alpha}(t) = x_{L,\alpha}(t + \Delta t) - x_{L,\alpha}(t) \tag{16}$$

where, Δt represents the order, which is greater than 1. The mathematical meaning of Eq.(16) is the difference value between t+Δt and t. When other behaviors of residential appliances occur during the charging duration, it is difficult to extract the start and end time. Therefore, how to set the value of Δt and ensure that identifying high-order difference points satisfy the constraints is the key to detect the edge of the charging behaviors.

Due to the high amplitude characteristic of the charging load, the point t can be regarded as the charging edge for $\Delta x_{L,\alpha}(t)$ exceeding a certain interval. In order to prevent certain high-power electrical appliances (such as AC) being mis-detected, it is necessary to introduce certain constraints for the charging load.

$$| \Delta x_{L,\alpha}(t) | \geq \eta \tag{17}$$

$$| \Delta x_{L,\alpha}^{+} + \Delta x_{L,\alpha}^{-} | \leq \varepsilon \tag{18}$$

$$Dur_{\min} \leq | t^{+} - t^{-} | \leq Dur_{\max} \tag{19}$$

$$\sum_{t=1}^{T} binary(t^{+} - t^{-}) \leq \Theta \tag{20}$$

where, t^+, t^- respectively represent rising edge and falling edge in $x_{L,\alpha}$; η donates the minimum difference, ε is the maximum asymmetry value. Eqs. (17-19) are the differential amplitude constraints, the symmetry constraints of the start and end edges of the charging event, and the interval constraints of the charging event, respectively. Eq. (20) is the constraint for the total number of charging events during T.

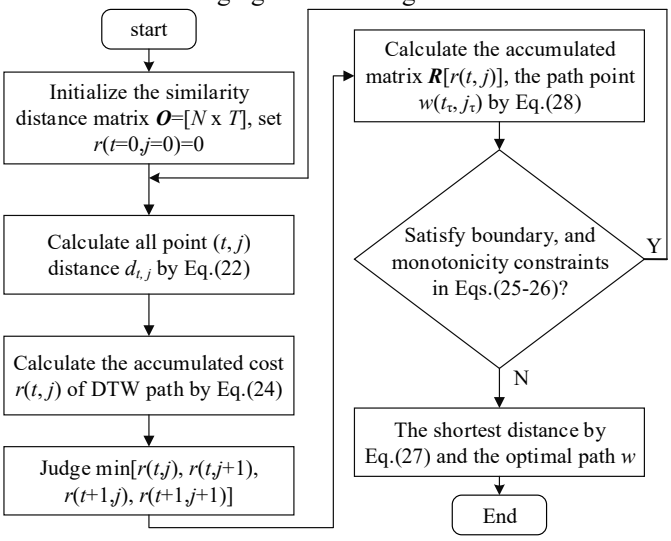

Fig. 4. Flowchart of the DTW algorithm

2) Matching the magnitude of the charging event

DTW is used to calculate the similarity between time series of different scales [29], which is mainly used for the charging load patterns matching. It describes the time corresponding relationship between the charging load template and the REV charging characteristic through the time warping function. Specifically, two unequal-length sequences are matched by solving the warping function corresponding to the smallest cumulative distance.

As can be seen from Section II, REV is mainly selected from M selectable patterns, where S=[s_1,…,s_M] represents the rated power vectors of M charging loads. $E_{interval}$=[t^+, t^-] is the start and end time points identified in 1), so the total selectable charging load patterns x_{opt} can be expressed as:

$$x_{opt} = (S \cdot E)_{M \times N} \tag{21}$$

where N donates the scale of $E_{interval}$, E is [1, N] row vector of all $E_{interval}$. Therefore, the $x_{L,\alpha}$=[a_1,..,a_t,…,a_T]$_{1xT}$ of REV extracted in two-stage, $x_{opt,i}$=[$se_{i,1}$,…,$se_{i,j}$,…,$se_{i,N}$] represents i-th charging load pattern from S, so the similarity distance matrix $\boldsymbol{O}$=[$d_{1,1}$,…,$d_{t,j}$,…,$d_{T,N}$] in DTW between $x_{L,\alpha}$ and $x_{opt,i}$ can be expressed as:

$$d_{t,j} = (a_t - se_{i,j})^2 \tag{22}$$

where, $d_{t,j}$ represents the distance between point j in $x_{opt,i}$ and point t in $x_{L,\alpha}$. The similarity matrix $\boldsymbol{O}$ can build all pairwise distance between a_t and $se_{i,j}$ (such as Euclidean distance, Mahalanobis distance). Therefore, the goal of the DTW algorithm is to find an optimal path W=[w_1,…,w_τ,…,w_k] from $\boldsymbol{O}$, which ensures $x_{L,\alpha}$ matches $x_{opt,i}$ to the maximum, and k should satisfy boundary constraint:

$$\max(T, N) \leq k \leq T + N - 1 \tag{23}$$

where, w_τ=(t_τ, j_τ)$\in$ {1,2,…t_τ…, t}x{1,2,…j_τ…, j} donates that a_t matches $se_{i,j}$, which can be considered that the jth amplitude

template of charging load is closest to $x_{L,\alpha}$ at time t. Eq. (23) donates the length of W should not be greater than the dimension of $\boldsymbol{O}$.The accumulated cost of DTW path W can be donated as:

$$r(t,j)=\sum_{\tau=1}^{k} d(t_\tau, j_\tau) \tag{24}$$

where $\tau \in \{1,2,\ldots,k\}$, and $r(t, j)$ represents the path length. Moreover, w_τ should satisfy the following constraints:

$$w_1=(1,1);\ w_k=(T,N) \tag{25}$$

$$\begin{cases} w_\tau=(t_\tau, j_\tau); w_{\tau+1}=(t_{\tau+1}, j_{\tau+1}) \\ 0 \le t_{\tau+1}-t_\tau \le 1 \\ 0 \le j_{\tau+1}-j_\tau \le 1 \end{cases} \tag{26}$$

Eqs. (25) and (26) are boundary constraint and monotonicity constraint for the w_τ, respectively. Besides, the continuity should be promised for any paths, that is, if the path has passed (t, j), then the next point can only be selected from $(t+1, j)$, $(t, j+1)$, $(t+1, j+1)$. Therefore, the DTW path is the shortest path that the w_τ satisfies the constraints of Eqs. (25-26), then the optimization goal of the DTW algorithm can be expressed as follows:

$$DTW(x_{L,\alpha}, x_{opt,i})=\min\left(\frac{1}{k}\sqrt{\sum_{\tau=1}^{k} w_\tau}\right) \tag{27}$$

The search for the optimal path is achieved through dynamic programming in term of the recursive process, and the specific process can be found in [30]. Besides, the shortest path is recorded by defining the accumulation matrix $R=[r(t, j)]_{T\times N}$, which can be expressed:

$$r(t,j)=d(t,j)+\min\begin{cases} r(t,j-1) \\ r(t-1,j) \\ r(t-1,j-1) \end{cases} \tag{28}$$

where, $r(0, 0)=0$; for t greater than 0, $r(t, 0)=\infty$; for j greater than 0, $r(0, j)=\infty$. After the accumulation matrix R is calculated by Eq. (28), the shortest distance and shortest path can be calculated according to Eq.(27). Anyway, the DTW algorithm finds the optimal (minimum distance) matching path while aligning two unequal length sequences, and the calculation process the DTW can be shown in Fig.4.

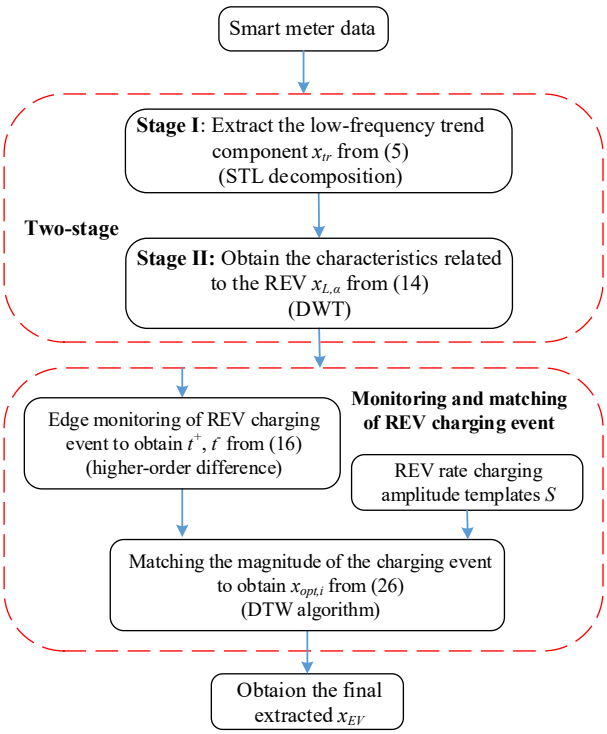

Fig. 5. Flowchart of the proposed algorithm

D.Flowchart and process illustration

The flowchart of the proposed method is presented in Fig. 5. First, the collected smart meter readings are decomposed into two stages. Smart meter data is decomposed into low-frequency trend components x_{tr} by STL decomposition in stage I. This process can eliminate the interference of high-frequency, residual, and periodic components. In stage II, the DWT algorithm is used to decompose x_{tr} into $x_{L,\alpha}$ related to the charging load profile. Stage II can effectively eliminate the interference of local noise components. Then, with the obtained $x_{L,\alpha}$, the edge monitoring (high-order difference) is adopted to extract the start and end time of the charging even t. Furthermore, combining the extracted charging time point and the REV amplitude template library, the DTW algorithm is used to calculate the optimal matching path between the amplitude template and $x_{L,\alpha}$, for determining the optimal charging amplitude.

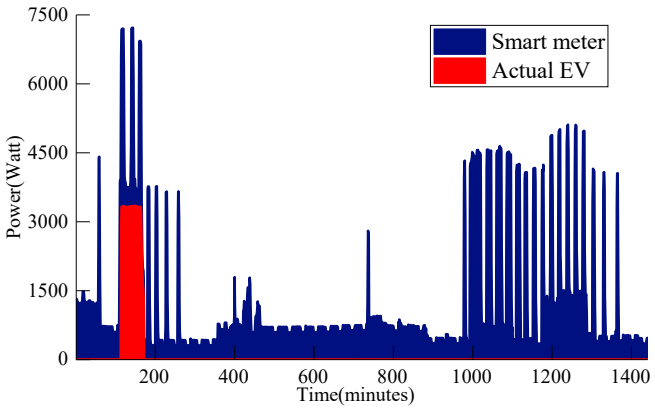

(a) Residential smart meter and EV data

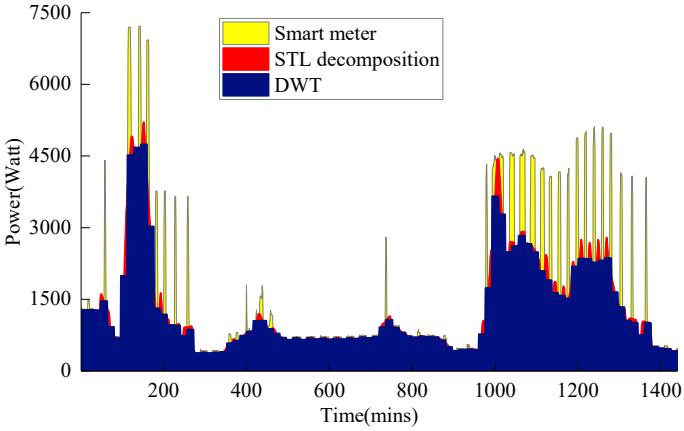

(b) Two-stage decomposition

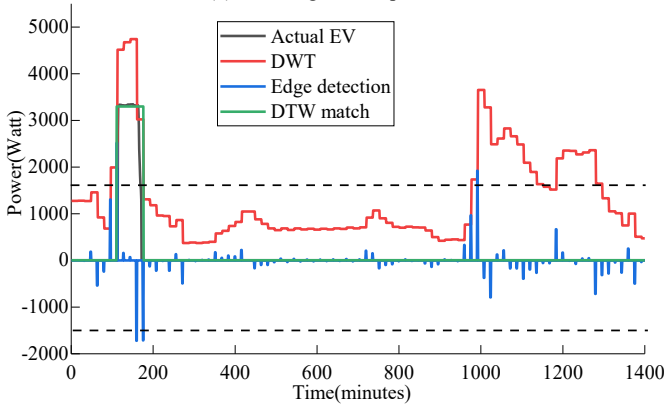

(c) Event detection and matching

Fig. 6. Process illustration

To further illustrate the effects achieved at each step in the flowchart, the smart meter data of household #1 in [7] (a day's household energy consumption) is used to show the effect of simple step decomposition. The smart meter data and actual EV power data of household #1 are shown in Fig. 6(a). The results of stage I (STL decomposition) and stage II (DWT) respectively in the two-stage decomposition are shown in Fig. 6(b). In Fig. 6(b), the high-frequency pulse components can be effectively eliminated after stage I, and there is a certain degree of agreement with the actual EV profile. The main reason is that STL decomposition can eliminate high-frequency cycles and random residual components. The local noise component of the trend component in stage I can be eliminated in stage II to a certain extent and the correlation with the actual EV profile is improved. Based on the results of stage II, the profile in Fig. 6(c) is the result of the edge monitoring and DTW matching respectively. In Fig. 6(c), multiple signal mutation points can be monitored through edge monitoring, but due to the constraints (17)-(20), the mutation points of the charging events can be only extracted. Furthermore, combining the DTW matching algorithm can match the amplitude power closest to the actual EV charging behavior.

E. Performance Evaluation

To evaluate the performance of the extraction algorithm and its corresponding results, some indexes are introduced.

1) E_{var} (Explained Variance Score)*:*

E_{var} is the degree of dispersion of the variance between the extracted results and the actual samples, which can fully quantify the error between the extracted charging load pattern and the actual EV charging load data.

$$E_{var}=1-\frac{\sum_{t=1}^{T}((x_{EV,t}-x_{REV,t})-A(x_{EV,t}-x_{REV,t}))^2}{\sum_{t=1}^{T}(x_{REV,t}-x_{ave,t})^2} \tag{29}$$

where, $x_{ave,t}$ represents the average of the actual charging load power, and A donates the function of the average. The closer E_{var} is to 1, the closer between the extracted results and the actual data is.

2) R2 (R-squared)*:*

R2-squared indicates the degree of correlation between the extracted results and actual samples, which is suitable for the charging load with obvious characteristics (charging interval, amplitude, etc). The closer R2 is to 1, the closer the extraction results are to the actual samples.

$$mse=\frac{1}{n}\sum_{t=1}^{T}(x_{EV,t}-x_{REV,t})^2 \tag{30}$$

$$R2=1-\frac{mse}{(1/n)\sum_{t=1}^{T}(x_{EV,t}-x_{REV,t})} \tag{31}$$

where, *mse* donates the means a square error, which measures the deviation between the sample and the extracted value, n represents the total sample points.

3) F1 (F1 Score)*:*

F1 can evaluate the accuracy of the NILE algorithm for identifying the ON/OFF appliances, while the charging load can be approximated as the binary appliances [5], [31]. Therefore, the extracted results can be evaluated using F1.

$$F1=\frac{2(PRE+REC)}{PRE+REC} \tag{32}$$

$$PRE=\frac{TP}{TP+FP} \tag{33}$$

$$REC=\frac{TP}{TP+FN} \tag{34}$$

where, PRE and REC are measured for the performance of the NILE algorithm to extract positive charging events; FP represents the number of samples that were incorrectly extracted as charging events; TP represents the number of samples that were correctly extracted as charging events, and FN represents the number of samples that were incorrectly extracted as non-charging events. Besides, the closer F1 is to 1, the better the performance of the NILE algorithm.

IV. Verifications And Discussions

A. Data Description

To verify the effectiveness and advantage of the proposed method, two sets of actual smart meter data from [24] are adopted for testing. Dataset#1 consists of the power consumption data of all electrical appliances of 23 households within a certain day in 2016, in which the household #4, #5, #13, and, #23 did not have to charge loads; Dataset#2 consists of daily aggregated power measurements for 5 households that have EVs for a period of six months (May. 2017- Oct. 2017) in New York, which corresponds to about 460 daily load patterns. Dataset#1 and #2 have a resolution of 1min and 10 mins,

respectively. Then the charging load pattern would be extracted from the smart meter data of each household and the actual measured REV data of each household will be used to evaluate the performance of the proposed method in the following tests.

In the case study, some parameters of the proposed algorithm are restricted within a certain range. η can be set between [1000,1500], while Dur_{min} is set as 30 mins, and Dur_{max} is set as 180 mins, which can be adopted from the conclusion in EACL. The determination of the minimum range (30 min) and the maximum range (180 min) of the charging interval is the probability statistics of residential charging behavior.

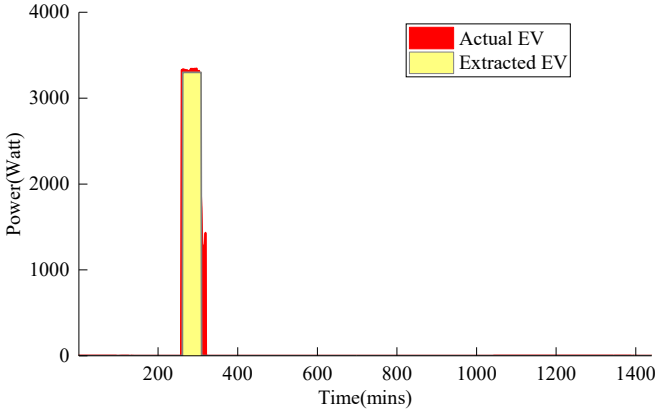

(a) Comparison of actual EV profile and extracted EV profile

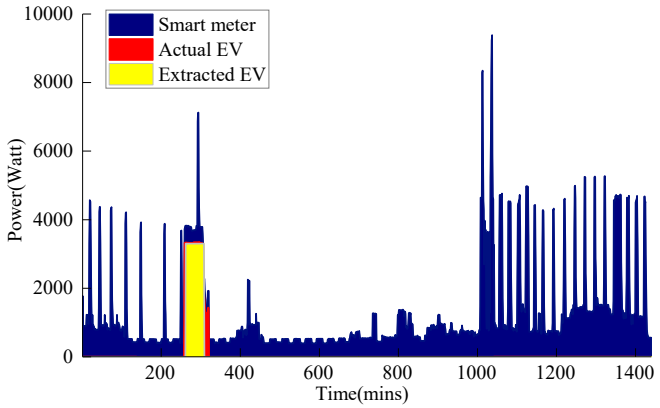

(b) Extraction by the proposed algorithm with the optimal parameters

Fig. 7. Extraction result analysis of household #15.

B. Testing and sensitivity analysis

The proposed method is tested on the selected dataset case and impacts of algorithm parameters on the extraction results are also investigated as a sensitivity analysis. Meanwhile, the optimal parameter set for the proposed algorithm will be selected with the best extraction performance.

Firstly, Dataset#1 is used to test the proposed algorithm with different parameters. The smart meter readings in Dataset#1 contain the superposition of various electrical appliances in a day, such as air conditioner, washing machine, and dryer. The key parameters that may affect the performance of the extraction are STL sampling frequency *freq*, DWT's architecture layers α, difference steps Δt, and η.

The sensitivity study aims to explore the impact of parameter settings on the performance of the proposed algorithm and explore the optimal parameter set as well. Table II shows the performance comparison of the proposed algorithm with different parameter settings. With different Δt, the values of E_{var}, R2, and F1 do not change significantly, which indicates that changing Δt has a limited effect on the extracted results. With the same η, the algorithm achieves the best performance when α=4 or 5. Besides, higher w leads to a better performance of the proposed algorithm.

TABLE II
PERFORMANCE COMPARISON WITH DIFFERENT PARAMETERS

Δt(mins)	η	*freq*	α	E_{var}	R2	F1
1	1000	24	3	0.755	0.804	0.790
	1000	24	4	0.884	0.907	0.931
	1000	24	5	0.884	0.907	0.931
	1000	24	6	0.667	0.725	0.780
2	1500	24	3	0.761	0.811	0.793
	1500	24	4	0.893	0.918	0.935
	1500	24	5	0.893	0.918	0.935
	1500	24	6	0.672	0.731	0.784

Moreover, the extraction results of household #15 based on the optimal parameters are shown in Fig. 7. The rectangular area (charging behavior) of charging load extraction in Fig.7 is similar to the actual charging load. Besides, we also conducted tuning experiments for other residents and found that the optimal parameter sets are consistent. Therefore, no extensive training or tuning process is required for the application of the proposed algorithm.

C. Comparative analysis using data in Dataset #1

The proposed algorithm is tested and compared with the pattern recognition and machine learning methods, e.g., FHMM [11], ASM[22], CNN[16].

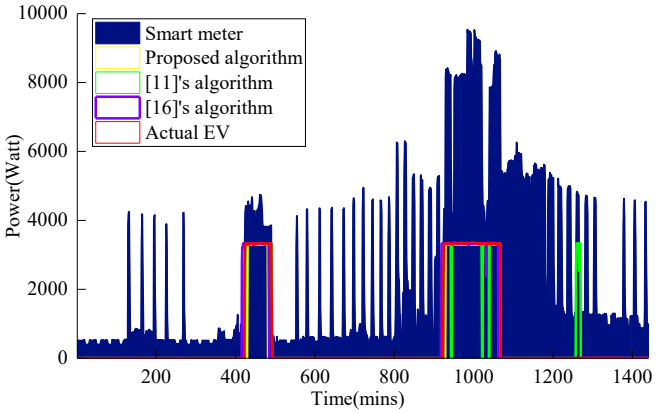

Fig. 8. Comparison with [11, 16], proposed algorithm in household #19

The charging load of all households in Dataset#1 are extracted by using the proposed algorithm and the algorithms in [11], [16], [22] and the performance results are shown in Table III. We find that the overall extracted performance of the proposed algorithm is better than those in [11] and [16], [22] for all households. We also illustrate the effectiveness of the proposed algorithm based on household #19 in Fig. 8, since the overlap between the charging load pattern and the power profile of the air conditioner, makes the charging load extraction extremely challenging. It is clear that the interval of charging behavior in household #19 is underestimated by the FHMM in [11], and an incorrect interval of the charging behavior is identified, which leads to low accuracy of extraction. When there is interference from high-frequency electrical appliances, the interval of charging behavior is overestimated by FHMM.

The main reason is that the high-frequency amplitude near the charging interval is mistaken as part of the charging load. The extracted results based on CNN in [16] are similar to the proposed algorithm because of the strong nonlinear fitting ability of CNN. However, since the CNN in [16] belongs to supervised learning, the training accuracy is directly linked to the amount of available data. In practice, it is difficult to obtain a large number of labelled sets (historical electric vehicle charging power data). For CNN, the convolution kernel is used to extract spatial feature, but the autocorrelation of timeseries is ignored.

TABLE III
PERFORMANCE COMPARISON OF THE ALGORITHM IN OVERALL DATASET#1

ID	Proposed algorithm		[11]'s algorithm		[16]'s algorithm		[22]'s algorithm	
	F1	E_{var}	F1	E_{var}	F1	E_{var}	F1	E_{var}
1	0.771	0.644	0.651	0.738	0.765	0.883	0.667	0.739
2	0.916	0.852	0.875	0.800	0.851	0.899	0.842	0.824
3	0.945	0.921	0.771	0.812	0.915	0.904	0.667	0.670
4	-	-	-	-	-	-	-	-
5	-	-	-	-	-	-	-	-
6	0.948	0.892	0.892	0.834	0.92	0.902	0.834	0.795
7	0.954	0.943	0.861	0.686	0.898	0.9	0.663	0.671
8	0.886	0.744	0.641	0.811	0.856	0.861	0.869	0.828
9	0.861	0.857	0.802	0.803	0.87	0.857	0.695	0.640
10	0.960	0.890	0.775	0.875	0.891	0.887	0.649	0.675
11	0.843	0.841	0.911	0.905	0.924	0.924	0.775	0.721
12	0.982	0.971	0.906	0.853	0.924	0.875	0.732	0.771
13	-	-	-	-	-	-	-	-
14	0.878	0.742	0.755	0.905	0.925	0.866	0.839	0.814
15	0.930	0.895	0.856	0.706	0.924	0.907	0.766	0.725
16	0.874	0.706	0.675	0.833	0.886	0.868	0.755	0.801
17	0.884	0.691	0.645	0.679	0.911	0.888	0.865	0.814
18	0.895	0.611	0.735	0.757	0.859	0.903	0.676	0.667
19	0.923	0.817	0.854	0.817	0.881	0.918	0.817	0.795
20	0.962	0.932	0.809	0.876	0.92	0.924	0.816	0.790
21	0.901	0.974	0.611	0.897	0.911	0.891	0.705	0.751
22	0.909	0.832	0.872	0.731	0.924	0.859	0.612	0.636
23	-	-	-	-	-	-	-	-

D. Spatial-temporal impacts on performance results

To further illustrate the performance of the proposed algorithm in dealing with seasonal data, the smart meter data of household #27 in Dataset#2 for 5 months (184 days) are considered for testing. The 2D kernel density map of the error value (1-R2) and the performance index (R2, E_{var}) of each month are shown in Fig.9, respectively.

The results in Fig. 9 show that the errors are concentrated around 0.2, demonstrating a consistent performance of the algorithm. However, in the worst case, the error value can get as large as 0.4. Besides, the performance in July and Aug tends to be worse than in other months. Owing to the power pattern of the air conditioner is similar to the charging load, which interferes with the extraction result. On the other hand, the best performance is achieved in Oct and May. In short, as the charging behavior and utilization of other appliances are affected by temperature in different seasons, the performance of the proposed algorithm may vary.

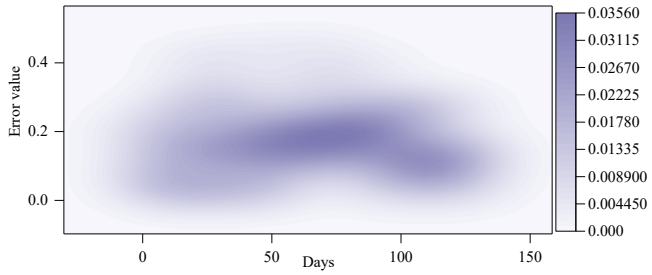

(a) Error's kernel density for 5 months

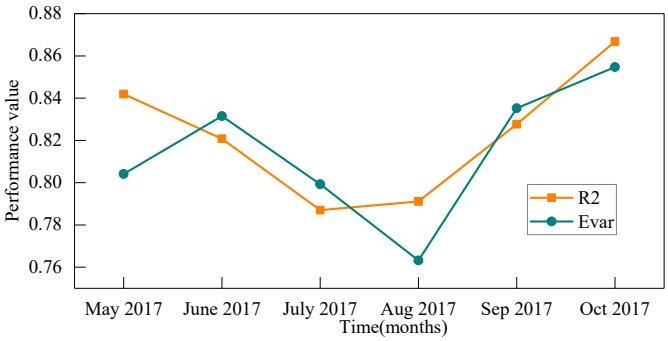

(b) Performance results for 5 months.

Fig. 9 The evaluation indexes result of household #27 in Dataset#2

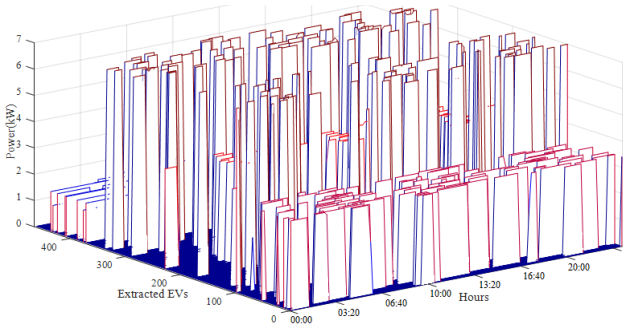

(a) Daily extracted EV patterns

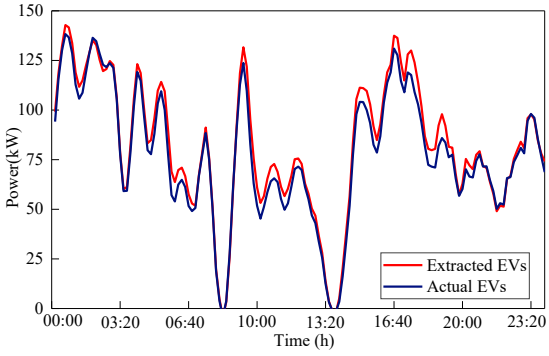

(b) Fitting of actual EVs profile in one day

Fig. 10. Extracted charging load patterns from Dataset#2

To further verify the performance of the proposed algorithm on different charging load profiles, the data for 5 households in Dataset#2 that have EV behavior for three months (May 2017-July 2017), which corresponding to about 460 (92 days*5 households) daily load patterns are considered. Besides, the 460 daily load patterns are investigated to avoid the sparseness of the charging load patterns by the 5 households in Dataset#2 for 3 months (May 2017-July 2017).

The daily extracted REV charging load patterns using the proposed algorithm are shown in Fig. 10(a). By accumulating all the daily charging load patterns extracted in Fig. 10(a) to one

day, and comparing it with the actual charging load profiles, the result can be as shown in Fig. 10(b) (accumulate 460 daily charging load patterns). For the charging load pattern extraction of those households, the purpose of Fig. 10(b) is to analyze the calculation error of the proposed algorithm for the application of aggregated EV charging load. The mean absolute error between the charging load pattern extracted by the algorithm and the actual charging load is only 2.513%.

E. The impact of noise on the proposed algorithm

The ability of noise immunity is an important issue in non-intrusive charging load extraction. Generally, noise exists throughout the life of data, and the main reasons include abnormal working conditions of electrical equipment, measurement errors, and privacy preservation mechanisms. Besides, microelectronics and high-frequency switching loads will mask the characteristics of the charging load pattern, which also could be considered as the noise. Existing research defaults that there is no noise interference in the smart meter data, so the robustness of the algorithm is not verified. In this case, the extraction results of the proposed algorithm, [11]'s, [16]'s, and [22]'s algorithm are compared after adding the noise signals of different sizes and shapes.

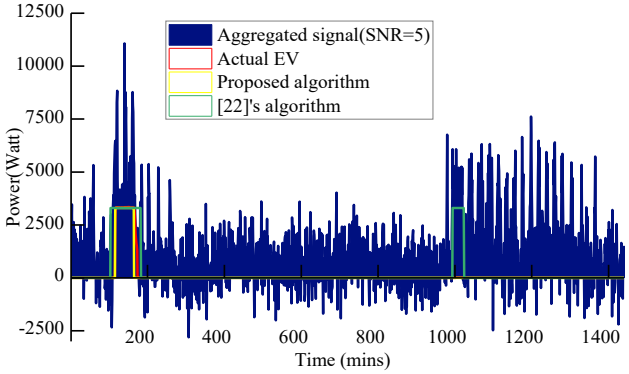

Fig. 11. Comparison of adding noise on household #1

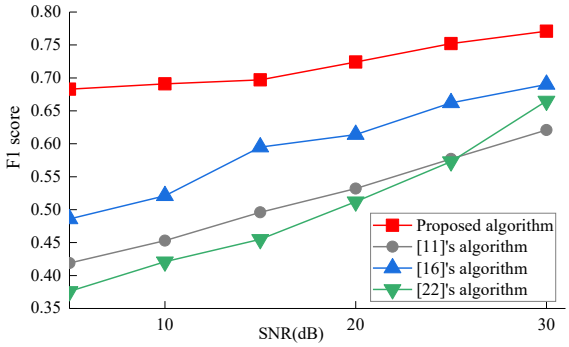

Fig. 12. Comparison of adding different SNR to household #1

The SNR is adopted to characterize the index of the size of the noise, and SNR = $10\log(x/x_{noise})$, where x and x_{noise} respectively represent the effective power of the smart meter and the noise signal. In general, the larger the SNR, the less the noise component mixed in the original signal. For the noise shape, we adopt Gaussian noise, Rayleigh noise, gamma noise, uniform noise, and impulse noise to analyze the effect of different types of noise on the results.

The extraction results after adding SNR = 5 (dB) white noise to household #1 can be shown in Fig. 11. The comparison of the F1 with different SNRs is shown in Fig. 12. The change of SNR has less influence on the extraction accuracy of the algorithm proposed in this paper. In particular, when SNR = 5dB, $F1$ is greater than 0.65, and when SNR = 30dB, the $F1$ is equal to the extraction result without added noise.

Since the two-stage decomposition method is adopted in the algorithm to extract characteristics related to the charging load, it is essentially a denoising process. Therefore, the training-free algorithm can accurate extraction of the charging load by adopting the frequency characteristics of different signals (low-frequency characteristics of charging load, random high-frequency characteristics of noise signals, etc.). On the contrary, the algorithms in [11] and [22] have a poor effect on charging loads with noise. When SNR = 5dB, the $F1$ value of the two is less than 0.45. For the FHMM in [11], the dictionary of noise signals is not considered when constructing the dictionary of base signals, which results in the extracted pattern containing noise components. As for the adaptive algorithm in [22], because the random signal and the smart meter data are superimposed, it is easy to generate an approximate charging interval, which is mistakenly judged as the charging load. The CNN in [16] has a powerful feature extraction function, which make the overall accuracy greater than [11], and [22]. However, the charging load characteristics are over-masked as the SNR decreases, resulting in the accuracy of CNN to decreases.

Due to the impacts of different shapes of noise on the results, the consistency of the basic parameters of different noise needs to be met. Therefore, the random functions in Python are adopted to generate Gaussian, uniform, erlang, rayleigh, and salt & pepper noise with values [-3000,3000], and variance is 0.5. The test results for different noise shapes can be seen in Fig.13.

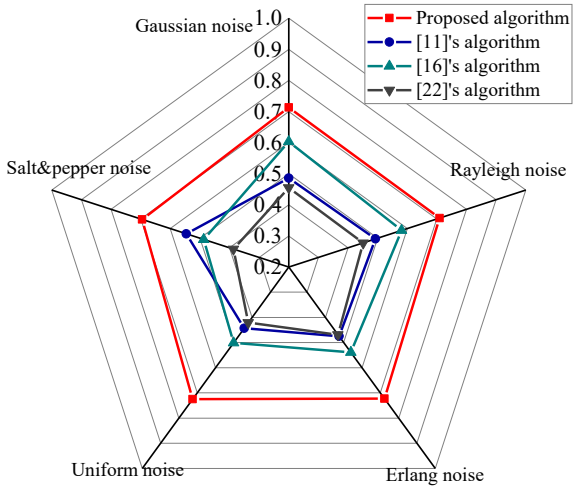

Fig. 13. Comparison of adding different shapes to household #1

In Fig. 13, the noise of different shapes has a small effect on the proposed algorithm, and the F1 value maintains at around 0.7. For different types of noise, which are essentially high-frequency components, and all can be filtered out by the algorithm. When the noise is salt & pepper noise, the $F1$ value of the algorithm in [22] is the smallest. The reason is that salt & pepper noise is similar to a pulse signal, and the algorithm in

[22] can misjudge it as a charging load. But for the algorithm in [11], salt&pepper noise can be approximated with the dictionary of other electrical appliances (switches), resulting in being extracted as the pattern of other electrical appliances. Due to the different overlapping effects of the charging load and the noise profiles, the amplitude of the charging load extracted by CNN in [16] is different.

F. The impact of data resolution on the proposed algorithm

In order to verify the performance of the proposed algorithm in terms of time resolution, Dataset#1 with a resolution of f=5, 10, and 15 minutes is considered. Note that the original resolution of Dataset#1 here is 1 minute, the household #4, #5, #13, and, #23 did not have to charge loads. The Evar index results of the proposed algorithm are shown in Table IV. In Table IV, the extraction accuracy of all households can be maintained at a high level, and as the sampling resolution f increases, the accuracy of the proposed algorithm in extracting the charging load pattern degrades. As the resolution f increases, the time complexity is reduced, and the charging load characteristics are lost. As a result, more accurate trend components cannot be obtained in the two-stage decomposition of the proposed algorithm. Since the proposed algorithm is designed based on the difference characteristics between the charging load and other electrical appliances, it has the ability of online identification and can extract the charging load pattern in a short time (less than 5s).

TABLE IV
RESULTS UNDER DIFFERENT SAMPLING RATES WITH PROPOSED ALGORITHM ON DATASET#1

ID	1	2	3	6	7	8	9
f=5	0.846	0.733	0.818	0.827	0.825	0.787	0.815
f=10	0.815	0.71	0.726	0.748	0.778	0.697	0.714
f=15	0.750	0.653	0.709	0.665	0.709	0.664	0.717
ID	10	11	12	14	15	16	17
f=5	0.821	0.834	0.820	0.848	0.792	0.786	0.827
f=10	0.815	0.796	0.762	0.757	0.74	0.765	0.765
f=15	0.672	0.66	0.665	0.71	0.691	0.688	0.717
ID	18	19	20	21	22		
f=5	0.831	0.846	0.806	0.829	0.802		
f=10	0.808	0.689	0.781	0.749	0.801		
f=15	0.667	0.704	0.704	0.675	0.689		

V. CONCLUSION

This paper introduces a novel NILE method to extract REV charging load patterns from the smart meter data. The proposed method adopts the low-frequency characteristics of the charging load and combines the feature extraction technology to reconstruct the REV charging load usage profiles. Data experiments show that compared with the existing NILE methods, the proposed method has the advantages of high accuracy and strong noise immunity. The parameter tuning of the proposed algorithm is simple, and the optimal parameters are universal. In future work, the robust of the algorithm could be investigated and aims to be improved with different resolutions of data.

REFERENCE

[1] Y. Xiang, S. Hu, "Electric vehicles in smart grid: a survey on charging load modelling," *IET Smart Grid*, vol. 2, no. 1, pp. 25-33, 2019.

[2] L, Wang, "The impact of plug-in hybrid electric vehicles on distribution network: a review and outlook," *Renew. Sust. Energ. Rev.*, vol. 15, no. 1, pp. 279-287, Oct. 2017.

[3] Y. Xiang, J. Liu, et. al, "Electric vehicle charging in smart grid: a spatial-temporal simulation method," *Energy*, vol. 189, pp. 166-221, 2019.

[4] Y. Xiang, J. Hong, et. al, "Development of EV charging templates: an improved K-prototypes method," *IET Gener. Transm. Distrib.*, vol. 12, no. 20, pp. 4361-4367, 2018.

[5] H. Zhao, X. Yan, et. al, "Training-free non-intrusive load extracting of residential electric vehicle charging loads," *IEEE Access*, vol. 7, 2019.

[6] P. Zhang, C. Zhou, G. S. Brian, "An improved non-intrusive load monitoring method for recognition of electric vehicle battery charging load," *Energy Procedia*, vol. 12 pp. 104-112, 2011.

[7] A. A. Munshi, A. R. I. Mohamed, "Extracting and defining flexibility of residential electrical vehicle charging loads," *IEEE Trans. Ind. Inf.*, vol. 14, no. 2, pp. 448-461, 2017.

[8] C. Nalmpantis, D. Vrakas, "Machine learning approaches for non-intrusive load monitoring: from qualitative to quantitative comparation," *Artif. Intell. Rev.*, vol. 52, no. 2, pp. 1-27, 2018.

[9] C. Zhou, S. Liu, P. Liu, "Neural network pattern recognition based non-intrusive load monitoring for a residential energy management system," *2016 3rd International Conference on Information Science and Control Engineering (ICISCE)*, *IEEE*, 2016.

[10] P. Francesca, P. Federica, et. al, "Context-based energy disaggregation in smart homes," *Future internet*, vol. 8, no. 1, pp. 4-26, 2016.

[11] M. Aiad, P. H. Lee. "Non-intrusive load disaggregation with adaptive estimations of devices main power effect and two ways interactions," *Energy Build.*, vol. 130, no. 15, pp. 131-139, 2016.

[12] J. Moragues, L. Vergara, J. Gosalbez. "Generalized matched subspace filter for non-independent noise based on ICA," *IEEE Trans. Signal Process.*, vol. 59, no. 7, pp. 3430-3434, 2011.

[13] A. Rahimpour, H. Qi, D. Fugate, "Non-intrusive energy disaggregation using non-negative matrix factorization with Sum-to-k constraint," *IEEE Trans. Power Syst.*, vol. 32, no. 6, pp. 4430-4441, 2017.

[14] S. Singh, "Deep sparse coding for non-intrusive load monitoring," *IEEE Trans. Smart Grid*, vol. 9, no. 5, pp. 4669-4678, 2017.

[15] M. Gupta, A. Majumdar. "Disaggregating transform learning for non-intrusive load monitoring," *IEEE Access*, vol. 6, pp. 46256-46265, 2018.

[16] D. Yang, X. Gao. Y. Pang, "An event-driven convolutional neural architecture for non-intrusive load monitoring of residential appliance," *IEEE Trans. Consum Electron*, vol. 66, no. 2, pp. 55-73, 2012.

[17] M. Figueiredo, A. D. Almeida, B. Ribeiro, "Home electrical signal disaggregation for non-intrusive load monitoring (NILM) systems," *Neurocomputing*, vol. 96, pp. 66–73, 2012.

[18] S. Alshareef, W. G. Morsi, "Application of wavelet-based ensemble tree classifier for non-intrusive load monitoring," *2015 IEEE Electrical Power and Energy Conference (EPEC)*, *IEEE*, 2015.

[19] J. Kim, T. Le, H. Kim, "Nonintrusive load monitoring based on advanced deep learning and novel signature," *Compu. Intell. Neurosci.*, pp.11-22, 2017.

[20] A. A. Munshi, Y. A. I. Mohamed, "Unsupervised nonintrusive extraction of electrical vehicle charging load patterns,", *IEEE Trans. Ind. Inf.*, vol. 15, no. 1, pp. 266–279, 2019.

[21] P. Zhang, C. Zhou, B. G Stewart, D. M Hepburn, W. Zhou, J. Yu, "An improved non-intrusive load monitoring method for recognition of electric vehicle battery charging load," *Energy Procedia*, vol. 12, pp. 104–112, 2011.

[22] Z. Zhang, et al., "Training-free non-intrusive load monitoring of electric vehicle charging with low sampling rate," *IEEE 40th Annual. Conf. IEEE Ind. Electron*, pp. 5418-5425, 2014.

[23] K. Qian, C. Zhou, M. Allan, "Modeling of load demand due to EV battery charging in distribution systems," *IEEE Trans. Power Syst.*, vol. 26, no. 2, pp. 802-810, 2011.

[24] (2019). *Pecan Street Inc. Dataport*. [Online]: Available: https://www.pecanstreet.org/.

[25] M. Muratori, M. C. Roberts, et. al, "A highly resolved modeling to simulate residential power demand," *Appl. Energy*, vol. 107, pp. 465-473, 2013.

[26] M. J. Sanchez-Vazquez, M. Nielen, et. al, "Using seasonal-trend decomposition based on loess (STL) to explore temporal patterns of pneumonic lesions in finishing pigs slaughtered in England," *Preventive Veterinary Medicine*, vol. 104, no. 1, pp. 65-73, 2012.

[27] W. S. Cleveland, "Robust locally weighted regression and smoothing scatterplots," *Publications of the American Statistical Association*, vol.

74, no. 368, pp. 829-936, 2014.
[28] J. M. Gillis, W. G. Morsi, "Non-intrusive load monitoring using semi-supervised machine learning and wavelet design," *IEEE Trans. Smart Grid*, vol. 8, no. 6, pp. 2648-2655, 2017.
[29] B. Liu, W. Luan, Y. Yu. "Dynamic time warping based non-intrusive load transient identification," *Appl. Energy*, vol. 195, no. 1, pp. 634-645, 2017.
[30] Y. Ge, J. M. Fitzpatrick, "On the generation of skeletons from discrete Euclidean distance maps," *IEEE Trans. Pattern Anal. Mach. Intell.*, vol. 18, no. 11, pp. 1056-1066.
[31] H. Liang, J. Ma, "Separation of residential space cooling usage from smart meter data," *IEEE Trans. Smart Grid*, vol. 11, no. 4, pp. 1-12, 2020.

Yue Xiang (SM'20) received the B.S. and Ph.D. degrees from Sichuan University, Chengdu, China, in 2010 and 2016, respectively. He was a Joint Ph.D. Student with the Department of Electrical Engineering and Computer Science, University of Tennessee, Knoxville, TN, USA, from 2013 to 2014. He was a Visiting Scholar with the Department of Electronic and Electrical Engineering, University of Bath, Bath, U.K., in 2015, and also a Visiting Researcher with the Department of Electrical and Electronic Engineering, Imperial College London, London, U.K., from 2019 to 2020. He is currently an Associate Professor with the College of Electrical Engineering, Sichuan University, Sichuan, China. His main research interests are distribution network planning and optimal operation, electric vehicle integration, and smart grid.

Yang Wang received the B.S. degree in electrical engineering and automation from Southwest Jiaotong University, China, in 2018 and the M.S. degree in electrical engineering with the Department of Electrical Engineering, Sichuan University, Chengdu, China, in 2021. He is currently working at the Powerchina Sichuan Electric Power Engineering Co., Ltd, Chengdu, China. His main research interests are distribution network planning, and smart grid.

Shiwei Xia (SM'20) received the B.Eng. and M.Eng. degrees in electrical engineering from Harbin Institute of Technology, Harbin, China, in 2007and 2009, respectively, and the Ph.D. degree in power systems from the Hong Kong Polytechnic University, Hung Hom, Hong Kong, in 2015. He then stayed with the department and worked as a Research Associate and subsequently as a Postdoctoral Fellow in 2015 and 2016. He was also a Visiting Faculty with the Robert W. Galvin Center for Electricity Innovation, Illinois Institute of Technology, Chicago, IL, USA, in 2019. Currently, he is with the State Key Laboratory of Alternate Electrical Power System with Renewable Energy Sources, School of Electrical and Electronic Engineering, North China Electric Power University, Beijing, China. His general research interests include security and risk analysis for power systems with renewable energies, distributed optimization and control of multiple sustainable energy sources in smart grid.

Tei Teng (M'15) received the BEng in Electrical Engineering from Beihang University, China, in 2009, and Ph.D. degree in Electrical Engineering from Imperial College London, U.K., in 2015. Currently, he is a Lecturer in the Department of Electrical and Electronic Engineering, Imperial College London, U.K. His research focuses on scheduling and market design for high power electronics penetrated systems, cyber-resilient energy system operation and control, and objective-based data analytics for future energy systems.